JB Journals.ASM.org

Regulation of the Min Cell Division Inhibition Complex by the Rcs Phosphorelay in *Proteus mirabilis*

Kristen E. Howery,[a] Katy M. Clemmer,[b] Emrah Şimşek,[c] Minsu Kim,[c] Philip N. Rather[a,b]

Department of Microbiology and Immunology, Emory University, Atlanta, Georgia, USA[a]; Research Service, Atlanta VA Medical Center, Decatur, Georgia, USA[b]; Department of Physics, Emory University, Atlanta, Georgia, USA[c]

ABSTRACT

A key regulator of swarming in *Proteus mirabilis* is the Rcs phosphorelay, which represses *flhDC*, encoding the master flagellar regulator $FlhD_4C_2$. Mutants in *rcsB*, the response regulator in the Rcs phosphorelay, hyperswarm on solid agar and differentiate into swarmer cells in liquid, demonstrating that this system also influences the expression of genes central to differentiation. To gain a further understanding of RcsB-regulated genes involved in swarmer cell differentiation, transcriptome sequencing (RNA-Seq) was used to examine the RcsB regulon. Among the 133 genes identified, *minC* and *minD*, encoding cell division inhibitors, were identified as RcsB-activated genes. A third gene, *minE*, was shown to be part of an operon with *minCD*. To examine *minCDE* regulation, the *min* promoter was identified by 5′ rapid amplification of cDNA ends (5′-RACE), and both transcriptional *lacZ* fusions and quantitative real-time reverse transcriptase (qRT) PCR were used to confirm that the *minCDE* operon was RcsB activated. Purified RcsB was capable of directly binding the *minC* promoter region. To determine the role of RcsB-mediated activation of *minCDE* in swarmer cell differentiation, a polar *minC* mutation was constructed. This mutant formed minicells during growth in liquid, produced shortened swarmer cells during differentiation, and exhibited decreased swarming motility.

IMPORTANCE

This work describes the regulation and role of the MinCDE cell division system in *P. mirabilis* swarming and swarmer cell elongation. Prior to this study, the mechanisms that inhibit cell division and allow swarmer cell elongation were unknown. In addition, this work outlines for the first time the RcsB regulon in *P. mirabilis*. Taken together, the data presented in this study begin to address how *P. mirabilis* elongates upon contact with a solid surface.

Proteus mirabilis, a Gram-negative member of the family *Enterobacteriaceae*, is a bacterium well known for its ability to swarm. Swarming is a specialized form of motility displayed by multicellular groups of flagellated bacteria across a solid or semisolid surface. In liquid culture, *P. mirabilis* exists as a peritrichously flagellated, rod-shaped cell. However, after coming into contact with a solid surface, the cells undergo differentiation into elongated, highly flagellated, multinucleate swarmer cells. Swarmer cells are 20- to 50-fold longer than vegetative cells and express thousands of flagella (1). Together, these swarmer cells form multicellular rafts, which they utilize to move across a solid surface (2). After a period of migration, the swarmer cells undergo consolidation (or dedifferentiation) and revert to vegetative rods. The repeated interchange from differentiation to consolidation is responsible for the characteristic bull's eye pattern that *P. mirabilis* forms on an agar plate (3, 4). Reviews on *P. mirabilis* swarming provide additional details on this process (5, 6).

The switch from a rod-shaped cell to a swarmer cell is a complex process involving several global regulatory factors. The regulator of colonic acid capsule synthesis (Rcs) phosphorelay is one of these important regulators. The Rcs phosphorelay consists of a sensor kinase (RcsC), a response regulator (RcsB), and a phosphotransferase (RcsD), which mediates the transfer of the phosphate from RcsC to RcsB (7, 8). An additional protein, RcsF, is an outer membrane lipoprotein that increases the levels of RcsC phosphorylation by some unknown mechanism (9). Once the system is activated, it results in phosphorylated RcsB, which represses *flhDC* (10). *flhDC* encodes the master regulator for flagellar synthesis, $FlhD_4C_2$, which controls genes central to flagellin production (11). The levels of *flhDC* increase in swarming cells (10, 12), and *flhDC* mutants do not swarm (10, 11). Factors that influence *flhDC* expression, such as activated RcsB, can have dramatic effects on the ability of *P. mirabilis* to swarm. When the Rcs system is active, for example, the cells exist as vegetative rods due to repression of *flhDC*; however, in *rcs* mutants, *P. mirabilis* cells hyperswarm due, in part, to increased *flhDC* expression (10, 13, 14). Another interesting phenotype of *rcs* mutants in *P. mirabilis* is the ability of cells to differentiate into swarmer cells in liquid; this phenomenon does not occur in wild-type cells or in cells overexpressing *flhDC* (10, 13, 14), suggesting that other genes within the Rcs regulon are involved in swarmer cell elongation. The external factors that influence the expression of the Rcs phosphorelay and $FlhD_4C_2$, and subsequently the cycles of differentiation and consolidation, are unknown. Cell-to-cell contact (4, 15) and extracel-

Received 13 February 2015 Accepted 7 May 2015

Accepted manuscript posted online 18 May 2015

Citation Howery KE, Clemmer KM, Şimşek E, Kim M, Rather PN. 2015. Regulation of the Min cell division inhibition complex by the Rcs phosphorelay in *Proteus mirabilis*. J Bacteriol 197:2499–2507. doi:10.1128/JB.00094-15.

Editor: J. P. Armitage

Address correspondence to Philip N. Rather, prather@emory.edu.

doi:10.1128/JB.00094-15

TABLE 1 Strains and plasmids used in this study

Strain or plasmid	Description and/or genotype[a]	Source or reference
E. coli		
DH5α	λ^- ϕ80d*lacZ*ΔM15 Δ(*lacZYA-argF*)*U169 recA1 endA1 hsdR17*(r_K^- m_K^-) *supE44 thi-1 gyrA relA1*	Laboratory stock
CC118 λ*pir*	*araD139* Δ(*ara leu*)*7697* Δ*lacZ74 phoA*Δ*20 galE galK thi rpsE rpoB argE*(Am) *recA1*	37
SM10 λ*pir*	*thi thr leu tonA supE recA* RP4-2Tc::Mu Kan^r λ*pir*	38
BL21(DE3)	F^- *ompT hsdS*(r_B^- m_B^-) *gal dcm* (DE3)	Stratagene
P. mirabilis		
PM7002	Wild type; Tc^r	ATCC
HI4320	Wild type; Tc^r	39
PMKH1	PM7002 *minC*::Kan^r	This study
PMKM1	PM7002 *rcsB*::Str^r	10
PMKH4	PM7002 *minC*::Kan^r *rcsB*::Str^r	This study
PMKH5	PM7002 *minC*::Kan^r(pMinCDE)	This study
PMKH6	PM7002(pMinClacZ)	This study
PMKH7	PM7002 *rcsB*::Str^r(pMinClacZ)	This study
PMKM2	HI4320 *rcsB*::Str^r	This study
Plasmids		
pBluescriptII SK(−)	ColE1 replicon; *lacZ*α Amp^r	Stratagene
pBC	High copy number; Cm^r	Stratagene
pKNG101	R6K replicon; mob^+ $sacB^+R^+$ Str^r	40
pTrc99a	ColE1 replicon; *trcPO lacI*^{q} Amp^r	41
pQF50	pRO1600 replicon; *lacZ*α (promoterless); Amp^r	29
pET21a	T7 expression vector; Amp^r	Novagen
pRcsB	pKNG101::*rcsB* (internal fragment); Str^r	10
pMinC	pKNG101 *minC*::Kan^r Str^r	This study
pBCMinCDE	pBC *minCDE* Cm^r	This study
pMinCDE	pKNG101 *minCDE* Str^r	This study
pMinClacZ	pQF50 *minCp* Amp^r	This study
pETRcsB	pET21a *rcsB* Amp^r	This study

[a] Kan^r, kanamycin resistant; Tc^r, tetracycline resistant; Str^r, streptomycin resistant; Amp^r, ampicillin resistant; Cm^r, chloramphenicol resistant.

lular signaling (16) are among the hypothesized factors that could play a role in these genetic and morphological cycles.

In *Escherichia coli* and other members of the *Enterobacteriaceae*, RcsB activates genes involved in cell division (17, 18), cell wall synthesis (17, 18), and virulence (19) while repressing genes involved in motility (10, 20). The rationale for investigating genes regulated by the Rcs phosphorelay in *P. mirabilis* lies in the observation that *rcs* mutants hyperswarm on solid agar and differentiate into swarmer cells in liquid culture. Therefore, it is inferred that the Rcs phosphorelay regulates the expression of genes important for swarmer cell formation, including elongation. One subset of genes activated by RcsB in other bacteria is those involved in cell division (17, 18). However, the role of the cell division machinery in *P. mirabilis* swarmer cell formation has not been investigated.

Cell division in many prokaryotes is dictated by the placement of the FtsZ-mediated Z-ring (21), whose positioning is determined by a group of negative regulators known as the Min system. The Min system is comprised of three proteins, MinC, MinD, and MinE, whose oscillation prevents the formation of the Z-ring at the poles of a rod-shaped cell (22, 23). MinC acts as the effector of this system by preventing FtsZ polymerization (23, 24). MinD binds the cell membrane in an ATP-dependent manner (25), where it recruits MinC and activates it 25- to 50-fold (24). The ATPase activity of MinD, which causes it to disassociate with the cell membrane, is induced by MinE (26). This trait of MinE, along with its ability to suppress the activity of MinCD (27), restricts cell division inhibition to one pole at a time and is responsible for the oscillating nature of the complex. When MinE stimulates disassociation of the complex at one pole, MinD-ADP moves to the opposite pole, where it recruits MinC, and the process begins again. A *min* mutant produces anucleate minicells from the pole of a mother cell, which, as a result of minicell production, is slightly enlarged (28). Though cells elongate during cell division inhibition, the potential roles these three proteins play in swarmer cell formation and motility have not yet been investigated.

In this study, we elucidate the regulation and role of the Min system in *P. mirabilis* swarming. We found that a *minC*::Kan^r mutation resulted in aberrant cell division in both vegetative and swarmer cells and decreased swarming motility. Additionally, we identified the transcriptional start site of the *minCDE* operon and demonstrated that the region encompassing this start site is bound by RcsB, the response regulator in the Rcs phosphorelay. Overall, our data demonstrate that the cell division inhibition machinery contributes to swarmer cell formation and identify an important regulator of the Min system.

MATERIALS AND METHODS

Bacterial growth conditions. Except where indicated, *P. mirabilis* and *E. coli* strains (Table 1) were grown in modified Luria-Bertani (LB) broth (10 g tryptone, 5 g yeast extract, 5 g NaCl per liter) at 37°C with shaking at 250 rpm. All the strains were incubated at 37°C. *E. coli* strains were grown on 1.5% LB agar, and *P. mirabilis* strains were grown on 3.0% LB agar to prevent swarming. Antibiotic selection for *E. coli* contained the following concentrations: 100 μg/ml ampicillin, 20 μg/ml kanamycin, and 25 μg/ml

TABLE 2 Primer sequences used in this study

Primer	Sequence (5′→3′)	Purpose
minC-F	TTTTTCTAGATTTTTGAGCGAGGCCGGTAG	*minC* mutation
minC-R	TTTTGGATCCAGCGACTTGCCTGAATATTTTAGT	*minC* mutation
PminC-F	TTTTGTCGACGCGCGAGATCTAGCAACATT	*minC* promoter activity
PminC-R	TTTTGGATCCCCTGAGCTGCTGGCTTAGTT	*minC* promoter activity
GSP1	CCAATATTGACCAGCAATGGAAACT	5′-RACE
GSP2	ACACCATAAATATGTACATTACCGTCT	5′-RACE
minCSS-F	TTAAGAATTCCGCGAGATCTAGCAACATTGCA	DNA binding studies
minCSS2-F	TTAAGAATTCAGCGACTTGCCTGAATATTTTAGT	DNA binding studies
minCSS2-R	TTAAGAATTCAATGGGCGTGTTTGACATCT	DNA binding studies
abaI-F	AAGTTAATCGCTTCTTGCAG	DNA binding studies
abaI-R	AGCTTATGTGGTCGCTCAAG	DNA binding studies
minCDE-F	ATAATTAAAACACAGAGCC	Complementing strain
minCDE-R	CCAGATTATAGAAAATTTAC	Complementing strain
minCqRT-F	CCCAAGCGCCTCAATTTCTG	qRT-PCR studies
minCqRT-R	TTCCCACAACACGTAAGCCA	qRT-PCR studies
minDqRT-F	CCACCAACCCAGAAGTCTCC	qRT-PCR studies
minDqRT-R	CGGCCTGGATTATAGCGTGT	qRT-PCR studies
minEqRT-F	CGCGTAAAAAGTCGACAGCA	qRT-PCR studies
minEqRT-R	TAAGCTGGCTCAGTATCGCC	qRT-PCR studies
16S-F	GGCTCAGATTGAACGCTGGC	qRT-PCR studies
16S-R	CGAAGAGCCCCTGGTTTGG	qRT-PCR studies
flhD-F	TTGGTTAAGTTGGCTGAAAC	Semiquantitative RT-PCR
flhD-R	TTTGTAGCAGAGGTATCATG	Semiquantitative RT-PCR
minE-R	CTTAGGTGATTCTTCATTTTCAGG	Operon study
rcsB-F	ACAGTCTAGAGATCCGACAGTTGCTGTAGC	RcsB protein purification
rcsB-R	AGACGTCGACCGGGTTAATGATGATGATGATGGCTTTCTCCGTTAATTTCCTTATC	RcsB protein purification

streptomycin. *P. mirabilis* antibiotic selection used 300 μg/ml ampicillin, 20 μg/ml kanamycin, 35 μg/ml streptomycin, and 15 μg/ml tetracycline. When appropriate, a concentration of 12 μg/ml 5-bromo-4-chloro-3-indolyl-β-D-galactopyranoside (X-Gal) was used for the selection of blue or white colonies for both *E. coli* and *P. mirabilis*. For induction of protein expression, a concentration of 1 mM isopropyl-β-D-thiogalactopyranoside (IPTG) was used.

DNA manipulations and transformations. All PCR amplifications were done using Phusion Hot Start II high-fidelity DNA polymerase (Thermo Scientific) and verified by DNA sequencing. All ligations were performed using the Fast-Link DNA ligation kit (Epicentre). For electroporation of plasmids into both *E. coli* and *P. mirabilis*, 30 ml of cells was grown to an optical density at 600 nm (OD_{600}) of 0.3 to 0.5 in LB broth. The cells were pelleted by centrifugation at 3,000 × *g* for 5 min at 4°C before being washed twice with 1 ml of ice-cold 10% glycerol and resuspended in 60 μl of ice-cold 10% glycerol per electroporation. Electroporations were done in Bio-Rad Gene Pulser 0.2-cm-diameter cuvettes with a Bio-Rad MicroPulser electroporator. Cells were plated on the appropriate antibiotics after 1.5 h shaking at 250 rpm at 37°C. For *P. mirabilis* transformations, competent cells were incubated for 30 min with plasmid DNA on ice prior to electroporation. *P. mirabilis* electroporations were allowed to recover for 3 h.

Construction of strains. For bacterial conjugations, overnight cultures were washed 3 times in 1 ml of fresh LB broth. One hundred microliters of each strain was combined in a 1.5-ml microcentrifuge tube before being added to a predried 1.5% LB agar plate; 200 μl of each strain alone was added to separate plates to serve as controls. After 7 h of incubation at 37°C, the cells were resuspended in 4 ml LB broth. The mating mixture and the individual control strains were plated on 3% LB agar containing the appropriate antibiotics and incubated overnight at 37°C.

To construct a *minC* mutant, the *minC* gene was amplified using minC-F and minC-R primers (Table 2) and ligated into pBluescript SK (Stratagene) digested with XbaI and BamHI (New England BioLabs). The cloned *minC* gene was then mutagenized using an EZ-Tn*5* <Kan-2> TNP Transposome kit (Epicentre). A *minC*::EZ-Tn*5* insertion in the center of the *minC* gene at a position 387 bp into the 702-bp *minC* open reading frame (ORF) was identified by restriction enzyme analysis and confirmed by DNA sequencing. This is referred to here as *minC*::Kan^r. This was then subcloned into pKNG101, creating pMinC. pKNG101 is a suicide vector harboring streptomycin resistance, used to select for initial pKNG101 integration, and the *sacB* gene, which selects for the loss of pKNG101 in the presence of 10% sucrose. pMinC was maintained in *E. coli* SM10 λ*pir*. This strain was conjugated with wild-type PM7002, and selection for PM7002 harboring the Campbell-type insertion at the *minC* locus was done on LB plates containing tetracycline (15 μg/ml) and streptomycin (35 μg/ml). An exconjugant was grown in LB broth for only approximately 10 generations and then plated on LSW agar (10 g tryptone, 5 g yeast extract, 5 ml glycerol, and 20 g agar per liter) containing 10% sucrose and kanamycin to select for clones that had lost pMinC but contained the *minC* locus harboring the EZ-Tn*5* Kan^r insertion. Clones that were Str^s Kan^r and sucrose resistant were subjected to Southern blot analysis to confirm they harbored the *minC*::Kan^r mutation. One of these strains, PMKH1 (PM7002 *minC*::Kan^r), was used for subsequent experiments.

To construct PMKH4 (PM7002 *minC*::Kan^r *rcsB*::Str^r), SM10 pKNG101::*rcsB* containing an internal fragment of *rcsB* (10) was conjugated to PMKH1. Exconjugants that were resistant to tetracycline, kanamycin, and streptomycin were confirmed using Southern blot analysis as having a disruption in the *rcsB* gene.

To complement the *minC* mutation, the *minCDE* region was amplified from PM7002 genomic DNA using minCDE-F and minCDE-R (Table 2). The *minCDE*-containing fragment was cloned into the SmaI site of pBC, creating pBCMinCDE. *minCDE* was digested out of pBCMinCDE using BamHI and XhoI and cloned into the BamHI/SalI sites of pKNG101, creating pMinCDE (pKNG101 plus *minCDE*). pMinCDE was maintained in *E. coli* SM10 λpir and conjugated to PMKH1. Exconjugants that were resistant to tetracycline, kanamycin, and streptomycin were

confirmed using Southern blot analysis, and one of the clones, PMKH5, was used for subsequent experiments.

pMinClacZ was created by PCR amplification of the *minC* upstream region using PminC-F and PminC-R and ligating it into the BamHI and SalI sites of pQF50, a low-copy-number vector harboring a promoterless *lacZ* that can be used to quantify promoter activities (29). pMinClacZ was electroporated into *E. coli* DH5α, and clones were selected on LB agar plates containing X-Gal and ampicillin. One of these confirmed clones was purified using the Qiagen Plasmid Mini-Kit, and 5 μl of this DNA was used to electroporate PM7002 and PM7002 *rcsB*::Str^r, creating PMKH6 and PMKH7, respectively.

5′-RACE. 5′ rapid amplification of cDNA ends (5′-RACE) was performed on 1.5 μg of RNA isolated from PM7002 using the 5′-RACE system (Invitrogen) according to version 2.0 of the manufacturer's protocol. First-strand cDNA synthesis was performed using GSP1 (Table 2). PCR amplification of the dCTP-tailed cDNA was done using GSP2 (Table 2) and the provided abridged anchor primer. Nested-PCR amplification of the diluted PCR product was done with Phusion Hot Start II high-fidelity DNA polymerase (Thermo Scientific) using the provided abridged universal amplification primer (AUAP) and GSP2. The resulting product was ligated into the SmaI site of pBC.SK and transformed into *E. coli* DH5α. The transformant was plated on ampicillin and X-Gal, and white colonies that were confirmed to have the 5′-RACE-generated product were sequenced to identify the 5′ end of the *minC* gene.

Phase-contrast microscopy. All phase-contrast microscopy images were captured with an Infinity 2-1 charge-coupled-device (CCD) camera (Lumenera) using an Olympus BX51 microscope. For imaging liquid cultures, cells were grown to mid-log phase, and 1.5 μl was pipetted onto a glass slide (VWR International). A coverslip (VWR International) was placed on top of the culture, and images were taken at ×1,000 magnification using oil immersion. Swarm fronts were imaged by adding 650 μl of LB agar to CoverWell imaging chambers (1 by 20 mm by 2.3-mm depth) and then adding 4 μl of an overnight culture to the solidified agar. The cells were grown in a humidified environment at 37°C until they began to swarm. A coverslip was placed on top of the imaging chamber containing the swarming cells, and images were taken at ×1,000 magnification using oil immersion. When applicable, antibiotics and IPTG were added to the media.

β-Galactosidase assays. Overnight cultures were standardized to the same optical density before 300 μl of each culture was spread plated onto 1.5% LB agar containing ampicillin and incubated at 37°C for 2 or 4 h. After the appropriate incubation period, cells were harvested from agar plates using 2 ml of ice-cold LB broth, and 0.9 ml of the harvested culture was pelleted by centrifugation at 13,000 rpm for 4 min. The pelleted cells were placed on ice for 20 min before lysis using chloroform and 0.1% SDS. β-Galactosidase activity was quantified as described by Miller (30).

EMSA. Electrophoretic mobility shift assays (EMSAs) were performed on digoxigenin (DIG)-ddUTP-labeled probes created by PCR amplification using Phusion Hot Start II high-fidelity DNA polymerase (Thermo Scientific) and primers containing EcoRI recognition sites at their ends (Table 2). The amplified DNA was digested with EcoRI for 3 h at 37°C, cleaned up using a PCR purification kit (Qiagen), and boiled for 10 min. After boiling, the digested DNA was placed immediately on ice, and 250 ng was incubated with 1 μl DIG-11-dUTP (Roche), 1 mM dATP (Roche), 4 μl buffer B (6 mM Tris-HCl, 6 mM $MgCl_2$, 50 mM NaCl, pH 7.5), and 1 μl Klenow enzyme (Roche). The labeling reaction mixture was incubated at 37°C for 1 h, followed by a 10-min incubation at 65°C to heat inactivate the Klenow enzyme. After labeling, the probe was cleaned up using the PCR purification kit.

Binding reactions were done by incubating 0.5 μl of labeled probe with 10× binding buffer (500 mM Tris-HCl, 1 M NaCl, 1 mM EDTA, 0.5 μg/μl bovine serum albumin [BSA], 100 mM dithiothreitol [DTT]), 1 μg/μl poly(dI-dC), and 0 to 320 pmol of purified His-tagged RcsB (RcsB-His_6) brought to a final volume of 20 μl with molecular biology grade water (Fisher). The reaction mixtures were incubated for 30 min at room temperature before being loaded with 5× DNA loading dye on a prerun Mini-Protean 5% Tris-borate-EDTA (TBE) precast gel (Bio-Rad). The gel was run at 100 V for approximately 3 to 4 h at 4°C until the loading dye was no longer visible on the gel. The DNA was transferred onto a 0.22-μm nylon membrane (MagnaGraph) at 15 V with a 0.4-mA limit for 45 min using a Bio-Rad Transblot SD Semi-Dry transfer cell. The DNA was cross-linked to the membrane using a Stratagene cross-linker. Blocking reagent (10×; Roche) was prepared in maleate buffer (100 mM maleic acid [pH 7.5], 150 mM NaCl), and the membrane was blocked for 30 min at room temperature using 1 times blocking solution diluted in maleic acid wash buffer (maleate buffer with 0.3% Tween 20). The membrane was then incubated for 30 min with a 1:1,000 dilution of antidigoxigenin coupled to alkaline phosphatase (Roche) in maleic acid wash buffer. The membrane was washed twice for 15 min each time with maleic acid wash buffer. The membrane was equilibrated in detection buffer (100 mM Tris-HCl [pH 9.5], 100 mM NaCl) for 2 min and then incubated with 1 ml of a 1:10 dilution of CDP-Star (Roche) for 5 min. After briefly blotting the membrane with Whatman paper, it was placed in a sealable plastic bag and exposed to film.

Swarm assays. Overnight cultures were standardized to the same optical density, and 4 μl of each culture was pipetted onto the same predried 1.5% LB agar plate. The culture was allowed to dry into the LB plate before being incubated at 37°C. Measurements of the swarm diameter in centimeters were taken every 30 min until the cells reached consolidation. Antibiotics were included in the agar plate when appropriate. The values represent the average diameter of duplicate sets (4 in total) with standard deviations.

Transcriptome sequencing (RNA-Seq). HI4320 and *rcsB*::Str^r (PMKM2) cells were harvested at an OD_{600} of 1.1 in triplicate. RNAprotect bacterial reagent was used at a 1:1 ratio (Qiagen). Total RNA was isolated using a MasterPure RNA purification kit (Epicentre), and contaminating DNA was removed using a Turbo DNA-Free kit (Ambion). RNA purity was confirmed on an Agilent 2100 bioanalyzer (Agilent Technologies). DNA-free samples were then enriched for mRNA using a MicrobExpress bacterial mRNA enrichment kit (Ambion). Two rounds of rRNA depletion were performed, and RNA purity was confirmed on an Agilent 2100 Bioanalyzer (Agilent Technologies). cDNA libraries were constructed from HI4320 and *rcsB*::Str^r mRNA using the SuperScript double-stranded cDNA synthesis kit (Invitrogen). The cDNA libraries were purified by phenol extraction and ethanol precipitation. Sequences were analyzed on an Illumina HiSeq2000 instrument with 50-bp paired-end reads and matched to the HI4320 genome using CLC Genomics Workbench (CLC Bio-Qiagen, Aarhus, Denmark). The total number of reads mapped per transcript was determined and used to determine the reads per kilobase per million reads (RPKM). Three separate sets of RNA samples were analyzed, and the average of samples from two sets was used (data available on request).

qRT-PCR. The same RNA used for RNA-Seq was used for quantitative real-time reverse transcriptase (qRT) PCR. Briefly, the RNA was transcribed into cDNA using an iScript Selected cDNA synthesis kit (Bio-Rad) according to the manufacturer's instructions. qRT-PCR was performed using a 1:10 dilution of the generated cDNA in iQ SYBR green Supermix (Bio-Rad). The reaction was completed in an iCycler iQ Real-Time PCR detection system (Bio-Rad), and the values were normalized to 16S rRNA expression for each sample. The expression of *minC*, *minD*, and *minE* in HI4320 was calculated relative to PMKM2 (HI4320 *rcsB*::Str^r) using the $\Delta\Delta C_T$ method (31). The primers used to quantify the expression of each gene can be found in Table 2.

Semiquantitative RT-PCR. Total RNA was harvested at hourly intervals (T_1, T_2, T_4, and T_6) after placing the cells on 1.5% LB agar plates using a MasterPure RNA purification kit (Epicentre). The T_0 sample represents cells immediately before being placed on agar surfaces. Contaminating DNA was removed using a Turbo DNA-Free kit (Ambion). The purified RNA was transcribed into cDNA using an iScript Selected cDNA synthesis kit (Bio-Rad). PCR amplification was performed using 16S-F and 16S-R

(Table 2), and aliquots from the PCR mixture were taken after 5, 10, and 15 cycles in order to equilibrate cDNA samples relative to 16S rRNA expression. Once equilibrated, *minC* expression was examined using minC-F and minC-R (Table 2) and *flhD* expression was examined using flhD-F and flhD-R (Table 2) at cycles 20, 25, 30, and 35.

Western blot analysis. Overnight cultures grown to stationary phase in LB were equilibrated to the same optical density, and then 300 μl was spread onto 1.5% LB agar before incubation at 37°C for 5 h. The cells were gently resuspended in cold LB broth to the same optical density, and 1.5 ml was pelleted and stored at −80°C. The cell pellets were lysed using 400 μl CellLytic B cell lysis reagent (Sigma). Equivalent protein levels for each sample were confirmed using a Bradford assay. The cell lysates were resuspended at a 1:1 ratio in Laemmli sample buffer. Samples were run on a 12% Mini-Protean TGX (Bio-Rad) gel and transferred to a nitrocellulose membrane. The primary antibody used was rabbit anti-FlaA obtained from Robert Belas at the University of Maryland. The secondary antibody was ECL peroxidase-labeled anti-rabbit antibody (Life Sciences).

DAPI (4′,6-diamidino-2-phenylindole) staining and microscopy. Swarmer cells were harvested after 5 h of incubation on 1.5% LB agar and resuspended in 1× phosphate-buffered saline (PBS). The cell suspensions were chemically fixed by the addition of formaldehyde (Sigma) to a 3% (vol/vol) final concentration and incubated for 10 min by gentle rocking. The fixed bacteria were attached to a poly-L-lysine (Sigma-Aldrich)-coated coverglass and incubated with DAPI (AnaSpec, Inc.) at 2 μg/ml (final concentration) in 1× PBS for 5 min in the dark. The excess DAPI solution was removed by washing with 1× PBS. The entire staining procedure was performed at room temperature. The DAPI-stained cells were imaged at room temperature using phase-contrast light and wide-field fluorescence microscopy with an Olympus IX83 microscope. An oil immersion 100× objective and a standard DAPI filter were employed for microscopy. Images were acquired using a Neo 5.5 sCMOS camera (Andor) and MetaMorph software (Molecular Devices). The images were prepared for publication using ImageJ software (NIH).

RESULTS

The *minCDE* operon is positively regulated by RcsB. Mutations in *rcsB* result in a hyperswarming phenotype and differentiation into swarmer cells in liquid, indicating that RcsB regulates genes important for swarmer cell differentiation (10). To identify these genes, RNA-Seq was performed on RNA isolated from liquid cultures of *P. mirabilis* HI3420 and an isogenic *rcsB*::Str^r mutant derivative at an A_{600} of 1.1. At this optical density, cells of the *rcsB* mutant were highly elongated, in contrast to the short rods of wild-type cells. When a cutoff of 2-fold or greater was applied, 87 genes were found to be RcsB repressed and 46 were RcsB activated (data available on request). Among the RcsB-regulated genes, we were interested in those that might contribute to cell elongation and initially focused on cell division genes. Expression of the *ftsA* and *ftsZ* genes was reduced 2.4- and 3.3-fold, respectively, in the *rcsB* mutant. However, the essential nature of these genes precluded a direct analysis of their role in cell elongation during swarming. Therefore, we focused on the *minC* and *minD* genes encoding components of a cell division inhibition complex, where expression decreased 3.4- and 6.7-fold, respectively, in the *rcsB* mutant relative to wild-type cells. The *minE* gene, located immediately downstream of *minD*, was not identified in the RNA-Seq as RcsB regulated, which was surprising, as *minE* is part of an operon with *minCD* in other bacteria (32, 33). To determine if the *minCDE* genes formed an operon in *P. mirabilis*, a primer specific to *minE* was used to prime cDNA synthesis, and the cDNA was used in a PCR to amplify the *minC* to *minE* region. The *minC* to *minE* region was amplified using the cDNA, but no product was observed with the RNA only, indicating that the *minCDE* genes form an operon (data not shown).

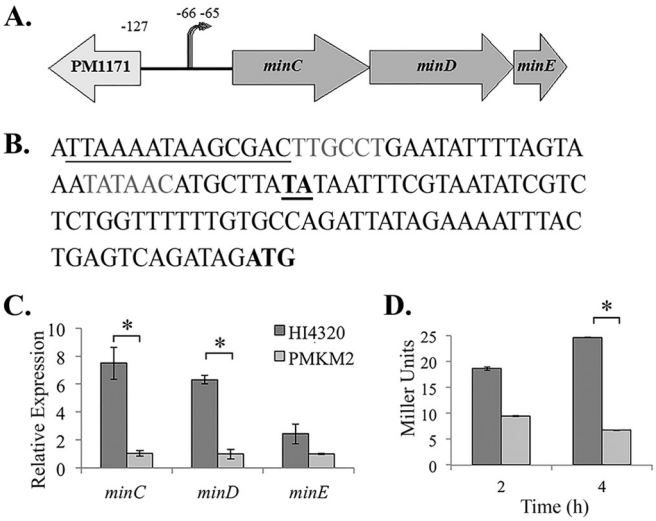

FIG 1 The *min* operon is positively regulated by RcsB. (A) Organization of the *minCDE* open reading frame. *minC* (702 bp), *minD* (813 bp), and *minE* (207 bp) are located in the same operon. The noncoding region upstream of *minC* is 127 bp long. Two transcriptional start sites for *minCDE* are located at positions −65 and −66 upstream of the *minC* start codon. (B) Sequence upstream of *minCDE*. The start codon of *minC* is in boldface. The two transcriptional start sites identified using 5′-RACE are underlined and in boldface. They are 65 and 66 bp upstream of the start codon. Upstream of the two identified start sites are putative −10 and −35 regions (gray letters). A potential RcsB binding site is underlined based on the *E. coli* consensus sequence (TAAGAATAATC CTA). (C) qRT-PCR analysis of *minC*, *minD*, and *minE* expression levels in *P. mirabilis* HI4320 and *P. mirabilis* HI4320 *rcsB*::Str^r (PMKM2). *minC* expression is 7.5 times lower in PMKM2 than in the wild type, *minD* expression is 6.3 times lower in PMKM2 than in the wild type, and *minE* expression is 2.4 times lower in PMKM2 than in the wild type. (D) β-Galactosidase activity of pMinCLacZ in the PM7002 wild type (PMKH6) (dark-gray bars) and PM7002 *rcsB*::Str^r (PMKH7) (light-gray bars). The activity of the *minC* promoter is decreased 2-fold in PMKH7 compared to PMKH6 after 2 h on solid agar and is decreased 4-fold in PMKH7 after 4 h on solid agar. The asterisks indicate a *P* value of <0.05.

To confirm the RNA-Seq data, the expression of *minC* and *minD* was examined by qRT-PCR using the same RNA used for RNA-Seq. A 7.4-fold decrease in *minC* expression was observed in the *rcsB* mutant relative to the wild type, and a 6.3-fold decrease in *minD* was observed (Fig. 1C). In addition, qRT-PCR analysis indicated that the expression of *minE* was reduced 2.4-fold in the *rcsB* mutant (Fig. 1C). These results indicate that RcsB positively regulates the *minCDE* operon.

Identification of the *minC* transcriptional start site and analysis of a *minC-lacZ* transcriptional fusion. The *minC* promoter region was identified by first determining the 5′ end of the *minC* mRNA using 5′-RACE with RNA harvested from wild-type PM7002. Two alternative transcriptional start sites were identified 65 and 66 bp upstream of the *minC* start codon. Upstream of the identified start sites were putative −10 and −35 regions and a possible RcsB binding site based on the *E. coli* consensus sequence AAGAATAATCCTA (Fig. 1B). To confirm that this region represented the *min* promoter, a DNA fragment encompassing from −169 to +371 relative to the transcriptional start site and containing the putative −10 and −35 regions was amplified using PCR. This fragment was ligated into pQF50, a low-copy-number vector

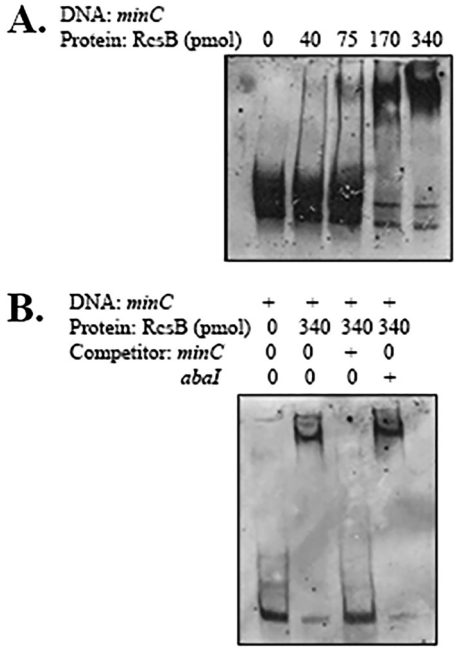

FIG 2 RcsB binds to the *minC* promoter region. Shown is binding of purified His-tagged RcsB to the *minC* upstream region. (A) Binding of the *minC* upstream region (290 bp) with increasing concentrations of RcsB. Lane 1 (from left), free labeled *minC* probe; lane 2, *minC* probe with 40 pmol RcsB; lane 3, *minC* probe with 75 pmol RcsB; lane 4, *minC* probe with 170 pmol RcsB; lane 5, *minC* probe with 340 pmol RcsB. (B) The digoxigenin-labeled 290-bp fragment was incubated with 340 pmol His-tagged RcsB. The binding was competed with unlabeled *minC* DNA (290 bp) and unlabeled *abaI* DNA (249 bp). Lane 1 (from left), free *minC* probe without RcsB or competitor; lane 2, *minC* probe with 340 pmol RcsB; lane 3, *minC* probe with 340 pmol RcsB and unlabeled *minC* DNA; lane 4, *minC* probe with 340 pmol RcsB and unlabeled *abaI* DNA.

harboring a promoterless *lacZ* gene (29), in order to quantify the *minC* promoter activity. The construct, pMinClacZ, was transformed into PM7002 and PM7002 *rcsB*::Str^r, and cells were collected after 2 (T_2) and 4 (T_4) h of incubation on agar plates at 37°C. The expression of β-galactosidase from pMinClacZ was 2-fold lower in the *rcsB* mutant at T_2 than in the wild type and was approximately 4-fold lower at T_4 (Fig. 1D).

RcsB directly regulates *minCDE* expression. The above-mentioned data indicated that RcsB positively regulated *minCDE* expression. Next, to determine whether RcsB exerted its effect on *minCDE* expression directly, EMSAs were performed using purified His-tagged RcsB and a 292-bp region upstream of *minCDE*. This 292-bp region included the transcriptional start site identified using 5′-RACE and extended from −208 to +82 relative to the transcriptional start site. A partial shift was observed when 75 pmol of RcsB was added to the reaction mixture, and this shift further increased at RcsB concentrations of 170 pmol and above (Fig. 2A). To confirm that the binding of RcsB was specific to the region upstream of *minC*, a competitive EMSA was performed with the unlabeled 292-bp *minC* promoter fragment and a 249-bp fragment containing the *abaI* gene from *Acinetobacter nosocomialis* strain M2 using the abaI-F and abaI-R primers (Table 2). At a concentration 50 times that of the labeled *minC* fragment, the unlabeled *minC* DNA prevented a shift. However, the unlabeled 249-bp *abaI* fragment did not affect the shift of the labeled *minC* fragment (Fig. 2B). Together, these data indicate that RcsB binds the region containing the *minC* promoter and that this binding is specific.

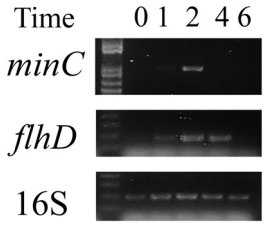

FIG 3 Semiquantitative RT-PCR of *minC*, *flhD*, and 16S RNA expression during swarmer cell differentiation. Total RNA was harvested at hourly intervals (T_1, T_2, T_4, and T_6) after placing cells on agar plates. The T_0 sample represents the cells immediately before being placed on agar surfaces. PCRs on cDNA samples prepared from RNA at each time point were amplified for 10 cycles (16S rRNA), 30 cycles (*minC*), or 25 cycles (*flhD*).

Expression of the *minCDE* operon during swarmer cell differentiation. To determine if *minCDE* expression varied during swarmer cell differentiation, expression was examined by semiquantitative RT-PCR from cells collected at hourly intervals after differentiation was initiated by placing the cells on agar plates. The expression of *minC* increased sharply by T_2 and then decreased to undetectable levels by T_4 (Fig. 3). As a marker for swarmer cell differentiation, *flhD* was also examined, and expression began to increase at T_1, peaked at T_2 to T_4, and then decreased by T_6 (Fig. 3).

A *minC* mutation results in aberrant cell division and minicell production. Since RcsB regulates genes important for swarmer cell differentiation, it seemed likely that the identification of the MinCDE cell division inhibitors as RcsB regulated indicated they probably had a role in swarmer cell elongation. To address the effect of the *min* system on *P. mirabilis* cell division and swarmer cell formation, a *minC*::Kan^r mutant was constructed. Cell morphologies were first examined in liquid media and imaged by phase-contrast microscopy. PM7002 produced short rod-shaped cells in liquid with an average length of 2.34 ± 0.6 μm (n = 147), while the *minC*::Kan^r mutant produced a typical *min* mutant phenotype with both enlarged cells and minicells, resulting in an average length of 3.72 ± 1.8 μm (n = 102) (Fig. 4). In contrast, no minicells were observed in wild-type cells. The *minC*::Kan^r mutation was complemented using the *minCDE* operon in single copy, as PMKH5 (PM7002 *minC*::Kan^r plus pMinCDE) shared the division phenotype of PM7002, with an average cell length of 2.37 ± 0.6 μm (n = 82) (Fig. 4).

The *minC*::Kan^r mutation reduces swarming motility. To investigate whether the *min* system was important for swarming in both wild-type and *rcsB*::Str^r mutant backgrounds, wild-type PM7002, a *minC*::Kan^r mutant, a *rcsB*::Str^r mutant, and the *minC*::Kan^r *rcsB*::Str^r double mutant were subjected to swarm assays. Measurements of the swarm diameter were taken every 30 min until the strains reached the first consolidation phase. PM7002 initiated swarming at approximately 4 h (T_4) after being spotted onto an agar plate (Fig. 5A). In contrast, the *minC*::Kan^r mutant experienced a half-hour delay in the onset of swarming and did not reach wild-type levels of swarming until the consolidation phase at T_6. The swarming phenotype of the *minC*::Kan^r mutant complemented with pMinCDE was not significantly different than that of the *minC*::Kan^r mutant alone (Fig. 5A), and the pos-

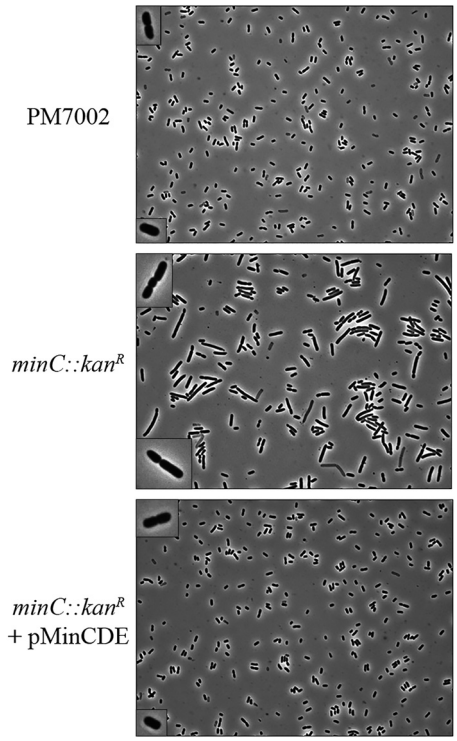

FIG 4 A *minC*::Kan^r mutation results in aberrant cell division in liquid culture. The cell division phenotypes for wild-type strain PM7002 (top), PMKH1 (PM7002 *minC*::Kan^r) (middle), and PMKH5 (PM7002 *minC*::Kan^r plus pMinCDE) (bottom) are shown. Cells were grown to mid-log phase, and 1.5 μl was imaged using phase-contrast microscopy. Liquid cultures of PM7002 exist as rod-shaped cells, often as doublets, with septa positioned at the centers of the cells. The *minC*::Kan^r mutation causes a large percentage of the cells to divide at the poles (middle image, insets). Minicells are often present. The division phenotype can be complemented by the addition of *minCDE* in single copy (bottom). The images were taken at ×1,000 magnification. All cell sizes in the insets have been increased equally.

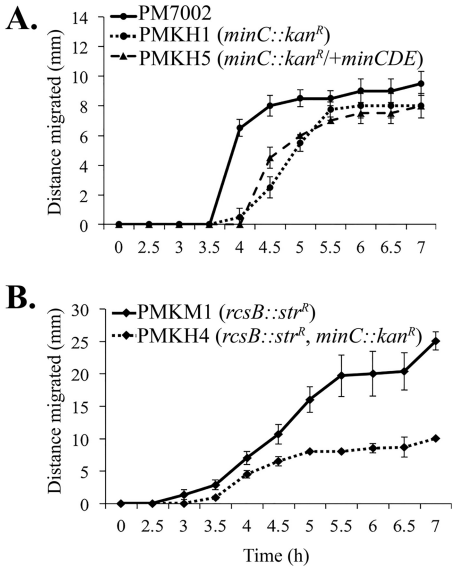

FIG 5 A *minC* mutation reduces *P. mirabilis* swarming in wild-type and *rcsB*::Str^r backgrounds. (A) The *minC*::Kan^r mutation was introduced into PM7002 (wild type) in order to create PMKH1 (PM7002 *minC*::Kan^r). The complementing strain was created by introducing pMinCDE (pKNG101 plus *minCDE*) into PMKH1. (B) The *minC*::Kan^r mutation was also introduced into PMKM1 (PM7002 *rcsB*::Str^r) in order to create PMKH4 (PM7002 *minC*::Kan^r *rcsB*::Str^r). All 5 strains were grown overnight in LB broth containing the appropriate antibiotics and then equilibrated to the same optical density. To investigate their abilities to swarm, 4-μl droplets of the equilibrated inocula were spotted onto the same plate, and the migration distance was measured every 30 min. The averages of four measurements are shown for PM7002, PMKH1, PMKM1, PMKH4, and PMKH5. The error bars indicate standard deviations.

sible basis for this is discussed below. As expected, the *rcsB* mutant hyperswarmed and initiated swarming an hour before the wild type (Fig. 5B). The *minC*::Kan^r *rcsB*::Str^r double mutant initiated swarming at the same time as the *rcsB*::Str^r mutant, but migration was 60% lower (Fig. 5B).

Since the *minC*::Kan^r mutation in both wild-type and *rcsB*::Str^r mutant backgrounds resulted in deficient swarming, the basis for this defect was examined by (i) analyzing the cell morphology at the swarm fronts, (ii) determining the levels of flagellin expressed in wild-type and *minC*::Kan^r mutant strains, and (iii) examining the nucleoid distribution in wild-type and *minC*::Kan^r mutant cells using DAPI staining. The PM7002 swarm front consisted of highly elongated, multinucleate swarm cells on the exterior and rod-shaped cells in the interior (Fig. 6A). In contrast, the *minC*::Kan^r mutant swarm front was a heterologous population of swollen and slightly elongated rod-shaped cells and minicells (Fig. 6A). The altered swarmer cell morphology at the swarm fronts of the *minC*::Kan^r mutant could be complemented by reintroducing the *minCDE* operon in single copy (Fig. 6A). The levels of flagellin (FlaA) detected by Western blotting were approximately 2-fold lower in the *minC*::Kan^r mutant at T_5 (Fig. 6B). However, complementation with pMinCDE did not restore flagellin expression in the *minC*::Kan^r mutant. In both the *minC*::Kan^r mutant and the complemented strain, the reduced flagellin likely contributes to the reduction in swarming. The basis for the ability of pMinCDE to complement the defect in cell morphology but not the reduced flagellin expression is unknown. There are no genes immediately downstream of *minCDE* in *P. mirabilis* that might have decreased expression due to a polar effect of the *minC*::Kan^r mutation or that could have been affected by introducing pMinCDE into the chromosome at the *min* locus. The lack of complementation with respect to swarming may have resulted from expression differences that failed to mimic the physiological level of MinCDE required for normal swarming but were able to rescue the morphological defect. For example, in *E. coli*, the *min* operon must be present at 1 to 10 times the physiological level in order to complement a *min* deletion mutant (32). Lastly, in both wild-type and *minC*::Kan^r mutant cells, multiple chromosomes typical of swarmer cells were present and were similar in appearance in each strain (Fig. 6C).

DISCUSSION

Previous studies have demonstrated that mutations that inactivate the Rcs phosphorelay in *P. mirabilis* result in hyperswarming on agar surfaces and constitutive swarmer cell formation in liquid media, a normally nonpermissive condition (10, 13, 14). The basis for the hyperswarming phenotype is due, in part, to the overexpression of the *flhDC* operon, which then activates genes involved in the production of flagella. However, overexpression of *flhDC* alone does not result in cell elongation, and therefore, the Rcs phosphorelay must also regulate genes involved in swarmer cell

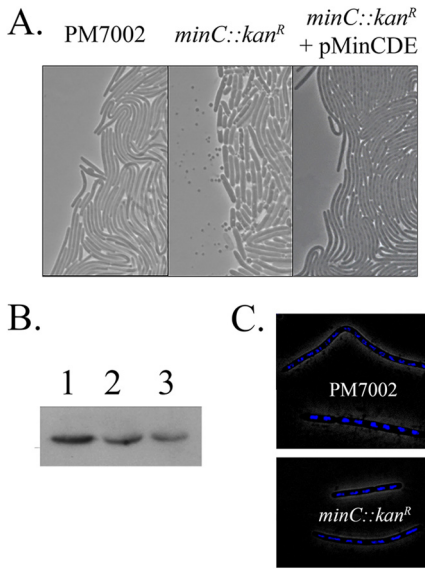

FIG 6 The *minC*::Kan^r mutation causes an atypical swarm front. (A) Stationary-phase cultures of PM7002 (wild type), PMKH1 (PM7002 *minC*::Kan^r), and PMKH5 (PM7002 *minC*::Kan^r plus pMinCDE) grown overnight in LB broth were equilibrated to the same optical density and then spotted onto 1.5% LB agar contained in a Coverwell imaging chamber. Once the cells began to swarm, phase-contrast images of PM7002 (left), PMKH1 (center), and PMKH5 (right) were taken of the swarm front at ×1,000 magnification. (B) Western blot analysis of flagellin (FlaA) expression in PM7002 wild-type (lane 1), PM7002 *minC*::Kan^r (lane 2), and PM7002 *minC*::Kan^r plus pMinCDE (lane 3) cells harvested after 5 h growth on LB agar plates. (C) DAPI staining of chromosomes in PM7002 (wild-type) and PMKH1 (PM7002 *minC*::Kan^r) swarmer cells.

elongation (10). Since *rcs* mutants constitutively elongate to swarmer cells in liquid media, this condition was chosen to identify RcsB-regulated genes that contributed to cell elongation by using RNA-Seq analysis. Based on this analysis, we chose to focus on two genes, *minC* and *minD*, that were activated by the Rcs phosphorelay and encoded components of the MinCDE cell division inhibition complex. Interestingly, a third gene, *minE*, which is typically cotranscribed with *minC* and *minD*, did not show up in the RNA-Seq analysis as RcsB regulated. However, our work demonstrated that *minE* was cotranscribed with *minCD* and thus that the three genes formed an operon. The inability to identify *minE* in the RNA-Seq analysis may have been due to reduced sensitivity of the technique compared to qRT-PCR, which showed a 2.4-fold reduction in the *rcsB* mutant (Fig. 1C). To confirm the activation of the *minCDE* operon by RcsB, a combination of transcriptional *lacZ* fusions and real-time PCR was used. In addition, purified RcsB was capable of binding the *minCDE* promoter region, indicating the regulation was direct. A possible RcsB binding site (TA AGAATAATCCTA) was present immediately upstream of the −35 region of the promoter (Fig. 1B). Additional studies, including mutagenesis of this putative RcsB binding site or demonstrating its ability to confer RcsB-dependent regulation on a heterologous promoter, will be needed to confirm the role of the sequence in RcsB binding.

Identification of the MinCDE cell division inhibition complex as regulated by the Rcs phosphorelay prompted our investigation of its function in swarmer cell elongation and swarming motility. We hypothesized that the expression of *minCDE* had to be tightly regulated during swarmer cell differentiation. During swarmer cell differentiation, there is a sharp increase in *minCDE* expression approximately 2 h after contact with an agar surface (T_2), and the increased levels of MinCDE likely contributed to the inhibition of cell division (Fig. 3). Consistent with this, we have observed that even slight increases in *minCDE* expression from an IPTG-inducible promoter resulted in a block in cell division and the formation of highly elongated cells (data not shown). Then, as the activity of the Rcs phosphorelay begins to decrease at T_3, the resulting decrease in levels of MinCDE would partially alleviate the block in cell division and allow cells to prepare for the consolidation phase, when they divide again. Consistent with this, a *minC* mutant was unable to elongate normally during swarmer cell differentiation and formed shorter cells than the wild type (Fig. 6). In addition, the *minC* mutant did not swarm as efficiently as the wild type (Fig. 5). This decrease in swarming was likely due to the decreased flagellin expression and the abnormal morphology in the *minC* mutant, which may affect the ability of the cells to form multicellular rafts. For example, it has been shown that a *ccmA* mutant in *P. mirabilis* produces curved cells that cannot align properly to form rafts during swarming. The mutant is able to differentiate into elongated, C-shaped swarmer cells but is unable to swarm (34).

To our knowledge, this is the first study to investigate the contribution of a cell division system to swarmer cell differentiation in *P. mirabilis*. In other bacteria, a *minC* mutation was found to reduce motility in *Helicobacter pylori*, but the mutant was highly elongated in liquid culture, which the authors hypothesized was the cause of reduced motility (35). In contrast, a mutation in a *minE* homolog in the Gram-positive bacterium *Clostridium perfringens* resulted in hypermotility and hyperelongation (36). In *P. mirabilis*, a null allele in *minC*, the proprietor of cell division inhibition in the Min system, did not induce hyperelongation in liquid culture or on solid surfaces in our study. The difference seen between these studies and ours highlights the underlying complexities and varying roles of the Min system in different organisms.

ACKNOWLEDGMENTS

We are grateful to Robert Belas for providing the FlaA antibody.

This work was supported by a Merit Review award from the Department of Veterans Affairs and by a Research Career Scientist award (P.N.R.). K.E.H. is supported by the Burroughs Wellcome Fund's Molecules to Mankind program.

REFERENCES

1. **Hoeniger JFM.** 1965. Development of flagella by *Proteus mirabilis*. J Gen Microbiol **40:**29–42. http://dx.doi.org/10.1099/00221287-40-1-29.
2. **Jones BV, Young R, Mahenthiralingam E, Stickler DJ.** 2004. Ultrastructure of *Proteus mirabilis* swarmer cell rafts and role of swarming in catheter associated urinary tract infection. Infect Immun **72:**3941–3950. http://dx.doi.org/10.1128/IAI.72.7.3941-3950.2004.
3. **Rauprich O, Matsushita M, Weijer CJ, Siegert F, Esipov SE, Shapiro JA.** 1996. Periodic phenomena in *Proteus mirabilis* swarm colony development. J Bacteriol **178:**6525–6538.
4. **Williams FD, Schwarzhoff RH.** 1978. Nature of the swarming phenomenon in *Proteus*. Annu Rev Microbiol **32:**101–122. http://dx.doi.org/10.1146/annurev.mi.32.100178.000533.
5. **Armbruster CE, Mobley HLT.** 2012. Merging mythology and morphology: the multifaceted lifestyle of *Proteus mirabilis*. Nat Rev Microbiol **10:**743–754. http://dx.doi.org/10.1038/nrmicro2890.
6. **Rather PN.** 2005. Swarmer cell differentiation in *Proteus mirabilis*. Environ Microbiol **7:**1065–1073. http://dx.doi.org/10.1111/j.1462-2920.2005.00806.x.

7. **Stout V, Gottesman S.** 1990. RcsB and RcsC: a two-component regulator of capsule synthesis in *Escherichia coli*. J Bacteriol **172:**659–669.
8. **Takeda S, Fujisawa Y, Matsubara M, Aiba H, Mizuno T.** 2001. A novel feature of the multistep phosphorelay in *Escherichia coli*: a revised model of the RcsC→YojN→RcsB signalling pathway implicated in capsular synthesis and swarming behavior. Mol Microbiol **40:**440–450. http://dx.doi.org/10.1046/j.1365-2958.2001.02393.x.
9. **Gervais FG, Drapeau GR.** 1992. Identification, cloning, and characterization of *rcsF*, a new regulator gene for exopolysaccharide synthesis that suppresses the division mutation *ftsZ84* in *Escherichia coli* K-12. J Bacteriol **174:**8016–8022.
10. **Clemmer KM, Rather PN.** 2007. Regulation of *flhDC* expression in *Proteus mirabilis*. Res Microbiol **158:**295–302. http://dx.doi.org/10.1016/j.resmic.2006.11.010.
11. **Claret L, Hughes C.** 2000. Functions of the subunits of the $FlhD_2C_2$ transcriptional master regulator of bacterial flagellum biosynthesis and swarming. J Mol Biol **303:**467–478. http://dx.doi.org/10.1006/jmbi.2000.4149.
12. **Pearson MM, Rasko DA, Smith SN, Mobley HLT.** 2010. Transcriptome of swarming *Proteus mirabilis*. Infect Immun **78:**2834–2845. http://dx.doi.org/10.1128/IAI.01222-09.
13. **Belas R, Schneider R, Melch M.** 1998. Characterization of *Proteus mirabilis* precocious swarming mutants: identification of *rsbA*, encoding a regulator of swarming behavior. J Bacteriol **180:**6126–6139.
14. **Liaw SJ, Lia HC, Ho SW, Luh KT, Wang WB.** 2001. Characterisation of p-nitrophenylglycerol-resistant *Proteus mirabilis* super-swarming mutants. J Med Microbiol **50:**1039–1048.
15. **Belas R.** 1997. *Proteus mirabilis* and other swarming bacteria, p 183–219. *In* Shapiro J, Dworkin M (ed), Bacteria as multicellular organisms. Oxford University Press, New York, NY.
16. **Sturgill G, Rather PN.** 2004. Evidence that putrescine acts as an extracellular signal required for swarming in *Proteus mirabilis*. Mol Microbiol **51:**437–446. http://dx.doi.org/10.1046/j.1365-2958.2003.03835.x.
17. **Carballès F, Bertrand C, Bouche JP, Cam K.** 1999. Regulation of *Escherichia coli* cell division genes *ftsA* and *ftsZ* by the two-component system *rcsC-rcsB*. Mol Microbiol **34:**442–450. http://dx.doi.org/10.1046/j.1365-2958.1999.01605.x.
18. **Gervais FG, Phoenix P, Drapeau GR.** 1992. The *rcsB* gene, a positive regulator of colonic acid biosynthesis in *Escherichia coli*, is also an activator of *ftsZ* expression. J Bacteriol **174:**3964–3971.
19. **Detweiler CS, Monack DM, Brodsky IE, Mathew H, Falkow S.** 2003. *virK*, *somA* and *rcsC* are important for systemic *Salmonella enterica* serovar Typhimurium infection and cationic peptide resistance. Mol Microbiol **48:**385–400. http://dx.doi.org/10.1046/j.1365-2958.2003.03455.x.
20. **Francez-Charlot A, Laugel B, Van Gemert A, Dubarry N, Wiorowski F, Castanié-Cornet MP, Gutierrez C, Cam K.** 2003. RcsCDB His-Asp phosphorelay system negatively regulates the *flhDC* operon in *Escherichia coli*. Mol Microbiol **49:**823–832.
21. **Bi EF, Lutkenhaus J.** 1991. FtsZ ring structure associated with cell division in *Escherichia coli*. Nature **354:**161–164. http://dx.doi.org/10.1038/354161a0.
22. **Ward JE, Lutkenhaus J.** 1985. Overproduction of FtsZ induces minicell formation in *E. coli*. Cell **42:**941–949. http://dx.doi.org/10.1016/0092-8674(85)90290-9.
23. **de Boer PA, Crossley RE, Rothfield LI.** 1990. Central role for the *Escherichia coli minC* gene product in two different cell division-inhibition systems. Proc Natl Acad Sci U S A **87:**1129–1133. http://dx.doi.org/10.1073/pnas.87.3.1129.
24. **de Boer PA, Crossley RE, Rothfield LI.** 1992. Roles of MinC and MinD in the site-specific septation block mediated by the MinCDE system of *Escherichia coli*. J Bacteriol **174:**63–70.
25. **Hu Z, Gogol EP, Lutkenhaus J.** 2002. Dynamic assembly of MinD on phospholipid vesicles regulated by ATP and MinE. Proc Natl Acad Sci U S A **99:**6761–6766. http://dx.doi.org/10.1073/pnas.102059099.
26. **Hu Z, Lutkenhaus J.** 2001. Topological regulation of cell division in *E. coli* spatiotemporal oscillation of MinD requires stimulation of its ATPase by MinE and phospholipid. Mol Cell **7:**1337–1343. http://dx.doi.org/10.1016/S1097-2765(01)00273-8.
27. **Zhao CR, de Boer PA, Rothfield LI.** 1995. Proper placement of the *Escherichia coli* division site requires two functions that are associated with different domains of the MinE protein. Proc Natl Acad Sci U S A **92:**4313–4317. http://dx.doi.org/10.1073/pnas.92.10.4313.
28. **Adler HI, Fisher WD, Cohen A, Hardigree AA.** 1967. Miniature *Escherichia coli* cells deficient in DNA. Proc Natl Acad Sci U S A **57:**321–326. http://dx.doi.org/10.1073/pnas.57.2.321.
29. **Farinha MA, Kropinski AM.** 1990. Construction of broad-host-range plasmid vectors for easy visible selection and analysis of promoters. J Bacteriol **172:**3496–3499.
30. **Miller JH.** 1972. Experiments in molecular genetics. Cold Springs Harbor Laboratory, Cold Spring Harbor, NY.
31. **Livak KJ, Schmittgen TD.** 2001. Analysis of relative gene expression data using real-time quantitative PCR and the 2(-Delta Delta C(T)) method. Methods **25:**402–408. http://dx.doi.org/10.1006/meth.2001.1262.
32. **de Boer PA, Crossley RE, Rothfield LI.** 1988. Isolation and properties of *minB*, a complex genetic locus involved in correct placement of the division site in *Escherichia coli*. J Bacteriol **170:**2106–2112.
33. **de Boer PA, Crossley RE, Rothfield LI.** 1989. A division inhibitor and a topological specificity factor coded for by the minicell locus determine proper placement of the division septum in *E. coli*. Cell **56:**641–649. http://dx.doi.org/10.1016/0092-8674(89)90586-2.
34. **Hay NA, Tipper DJ, Gygi D, Hughes C.** 1999. A novel membrane protein influencing cell shape and multicellular swarming of *Proteus mirabilis*. J Bacteriol **181:**2008–2016.
35. **Chiou P, Luo C, Chang K, Lin N.** 2013. Maintenance of the cell morphology by MinC in *Helicobacter pylori*. PLoS One **8:**e71208. http://dx.doi.org/10.1371/journal.pone.0071208.
36. **Liu H, McCord KD, Howarth J, Popham DL, Jensen RV, Melville SB.** 2014. Hypermotility in *Clostridium perfringens* strain SM101 is due to spontaneous mutations in genes linked to cell division. J Bacteriol **196:**2405–2412. http://dx.doi.org/10.1128/JB.01614-14.
37. **Manoil C, Beckwith J.** 1985. TnphoA: a transposon probe for protein export signals. Proc Natl Acad Sci U S A **82:**8129–8133. http://dx.doi.org/10.1073/pnas.82.23.8129.
38. **Miller VL, Mekalanos JJ.** 1988. A novel suicide vector and its use in construction of insertion mutations: osmoregulation of outer membrane proteins and virulence determinants in *Vibrio cholerae* requires *toxR*. J Bacteriol **170:**2575–2583.
39. **Mobley HLT, Warren JW.** 1987. Urease-positive bacteriuria and obstruction of long-term urinary catheters. J Clin Microbiol **25:**2216–2217.
40. **Kaniga K, Delor I, Cornelis GR.** 1991. A wide-host-range suicide vector for improving reverse genetics in gram-negative bacteria: inactivation of the *blaA* gene in *Yersinia enterocolitica*. Gene **109:**137–141. http://dx.doi.org/10.1016/0378-1119(91)90599-7.
41. **Amann E, Ochs B, Abel KJ.** 1988. Tightly regulated tac promoter vectors useful for the expression of unfused and fused proteins in *Escherichia coli*. Gene **69:**301–315. http://dx.doi.org/10.1016/0378-1119(88)90440-4.